Inhibition of β-catenin Protects Mouse Hearts From Ventricular Arrhythmias After Myocardial Infarction Independent of Ion Channel Gene Changes

Jerry Wang
University of Ottawa Heart Institute
Ying Xia
University of Ottawa Heart Institute
Aizhu Lu
University of Ottawa Heart Institute
Hongwei Wang
University of Ottawa Heart Institute
Darryl R. Davis
University of Ottawa Heart Institute
Peter Liu
University of Ottawa Heart Institute
Rob S. Beanlands
University of Ottawa Heart Institute
Wenbin Liang (wlian3@uottawa.ca)
University of Ottawa

Research Article

Keywords: Ventricular arrhythmia, Myocardial infarction, Heart failure, Wnt signalling, β-catenin

Posted Date: April 12th, 2021

DOI: https://doi.org/10.21203/rs.3.rs-393358/v1

Abstract

The Wnt/β-catenin signaling regulates ion channel gene expressions in cardiomyocytes. Because Wnt/β-catenin signaling is activated in myocardial infarction (MI), this study aims to investigate if β-catenin inhibition affects post-MI ion channel gene alterations and ventricular tachycardias (VT). MI was induced by permanent ligation of left anterior descending artery in wild-type (WT) and cardiomyocyte-specific β-catenin knockout (KO) mice. KO mice showed reduced susceptibility to VT (18% vs. 77% in WT) at week-8 after MI, associated with attenuated structural remodeling (reduced scar size and attenuated left ventricle dilation) as compared to WT. However, at the subacute phase (week-1) and chronic phase (week-8) after MI, Wnt/β-catenin signaling activation was found in non-cardiomyocytes, but not in cardiomyocytes. Downregulations of *Scn5a* (encoding $Na_v1.5$) and *Gja1* (encoding Cx43) were found at week-1 but not at week-8, while downregulations of K^+ channel genes were present at both week-1 and -8. Consistent with no activation of Wnt/β-catenin pathway in cardiomyocytes at week-1 and -8, these alterations in ion channel/transporter genes were not different between KO and WT mice. This study demonstrated that mice with cardiomyocyte-specific β-catenin deletion have reduced VT susceptibility after MI which is caused by attenuated structural remodeling, instead of alterations in ion channel gene expressions.

Introduction

Each year, ventricular tachyarrhythmia-induced sudden cardiac death (SCD) claims the lives of millions of people worldwide, including ~370,000 Americans[1] and ~700,000 European people.[2] Ischemic heart disease (myocardial infarction, MI) is the most common underlying disorder and accounts for 65-80% of the SCD cases[3]. In post-MI hearts, ventricular tachyarrhythmias (including tachycardia and fibrillation, VT/VF)[4,5] result from both structural remodeling of the injured heart, i.e. fibrosis and scar formation in the infarcted region, and alterations in expression of ion channels/transporters especially in the border zone of the infarct,[6,7] such as reduced $Na_v1.5$[8] and Cx43[9] as well as re-distribution of Cx43 (less in intercalated disk, but more in lateral surface of myocytes)[9]. The scar tissues are often interspersed with bundles of survived cardiomyocytes, which form “reentry circuit” together with border zone myocardium that has reduced and heterogenous conduction velocity providing the substrate for VT/VF[6]. The alterations in ion channels in survived myocardium also increases their automaticity or triggered activity[10] that can initiate VT/VF.

The Wnt signaling is critical for embryonic cardiogenesis[11] and we have recently shown that it regulates the differentiation of embryonic stem cells into different subtypes of cardiomyocytes.[12] In the canonical Wnt/β-catenin pathway, the binding of Wnt ligands to their plasma membrane receptors leads to the cytoplasmic accumulation of β-catenin, followed by its translocation into the nucleus and activation or inhibition of the transcription of target genes. In healthy adult hearts, Wnt/β-catenin signaling has a low activity but recent studies have suggested that its activity is increased in the myocardium in both human ischemic heart failure[13] and animal models of myocardial infarction[14] and heart failure,[15] as well as in murine models of pressure overload-induced hypertrophy.[16,17] However, one study reported that increased

Wnt/β-catenin signalling was only found in the myocardium of post-MI pigs with hypercholesterolemia, but not in post-MI pigs with normal cholesterol levels.[18]

Recent studies, including those from our group,[19,20] have demonstrated the capability of Wnt/β-catenin signalling to regulate the expression of both *Scn5a (encoding* $Na_v1.5$)[19-24] and *Gja1* (encoding Cx43),[24,25] which are critical for the myocardial conduction velocity and play roles in post-MI electrical remodeling and arrhythmogenesis. However, it remains unknown if Wnt/β-catenin signalling plays a role in the post-MI alterations in ion channel genes.

On the other hand, previous studies have not reached a consensus regarding the role of Wnt/β-catenin signaling in the structural remodeling of the post-MI hearts. Several studies have suggested that the Wnt/β-catenin signaling is cardioprotective and reduces scar size. In post-MI rats, viral expression of a constitutively active form of β-catenin in the border zone reduced infarct size, which is associated with reduced apoptosis and increased cell proliferation in both cardiomyocytes and fibroblasts.[26] In mice with deletion of Lrp5, the co-receptor required for Wnt/β-catenin pathway activation, the infarct size after MI was larger than in wild-type mice.[18] In mice with fibroblast-specific deletion of β-catenin, ischemia/reperfusion injury induced accelerated LV dilation and pump dysfunction.[14] By contrast, other studies have suggested a detrimental role of Wnt/β-catenin signaling. In post-MI mice, enhancement of the Wnt/β-catenin signaling in myocardium via Wnt3a protein injection accentuated cardiac dysfunction by inhibition of cardiac progenitor cell proliferation and endogenous regeneration.[27] Mice overexpressing FrzA (Sfrp-1), an inhibitor of the Wnt signaling, had reduced scar size and cardiac rupture after MI, which are associated with reduced cell apoptosis in the scar region.[28] In mice with αMHC-Cre mediated β-catenin deletion, which made the cells non-responsive to Wnt stimulation, the scar size after MI was smaller which was associated with enhanced differentiation of a cardiac progenitor population (marked as αMHC+/TAGA4+/Tbx5+, but cTnT-) into small cTnT+ cardiomyocytes in the infarcted region.[29]

In the present study we demonstrated for the first time that mice with cardiomyocyte-specific deletion of β-catenin have reduced susceptibility to ventricular tachyarrhythmias at 8 weeks after MI, which is associated with attenuated structural remodeling, but without affecting ion channel gene expressions.

Results

β-catenin knockout reduces the susceptibility to ventricular tachycardias after myocardial infarction

Successful knockout of β-catenin after tamoxifen treatment was confirmed by western blot showing marked reductions of β-catenin protein in the left ventricle of *Ctnnb1*$^{flox/flox}$;αMHC-MerCreMer$^{+/-}$ (KO) mice as compared to *Ctnnb1*$^{flox/flox}$;αMHC-MerCreMer$^{-/-}$ (WT) mice (Figure 1A, 1B and 1C). Post-MI survival curve showed that there was no difference (p=0.75) in the death rate between WT and KO groups (Figure 1D) with all the death (15% for WT; 19% for KO) occurred within the first week in both groups. The absence of animal deaths in the late stage after MI suggests no lethal arrhythmias in these mice. This

reflects a known limitation of studying arrhythmias in mice—the low rates of spontaneous arrhythmias due to their fast heart rate, short action potential duration and smaller heart size, as compared to human and large animal models (e.g., monkeys and pigs) of heart disease.

To investigate the susceptibility of mice to ventricular arrhythmias, we used a protocol that we recently developed for rodent hearts[20,30] that combined adrenergic stimulation (with isoproterenol) and progressive programmed electrical stimulation (PES) in isolated, Langendorff-perfused hearts (Figure 1E), while *ex vivo* ECG was recorded by placing electrodes around the heart. With this protocol, ventricular tachycardias (VT, defined as three or more consecutive ectopic ventricular beats) were successfully induced in 77% (10/13) post-MI WT mice at week 8, but in none (0/18) of the sham-operated WT mice (Figure 1F and 1G) validating our VT-inducing protocol. No difference was observed between male and female mice in VT inducibility (4/5 in male and 6/8 in female, p=0.84) or arrhythmia score (Figure 1G) (3.40±0.60 in male and 3.13±0.58 in female, p=0.76). In contrast, VT was induced in only 18% (2/11) of the post-MI KO mice at week 8 indicating reduced susceptibility to ventricular arrhythmias ($p<0.05$ vs. WT, Figure 1G,). Interestingly, a significant portion of the KO mice at week 8 after MI (55% vs. 15% in WT) exhibited isolated or coupled premature ventricular contractions (PVCs) that did not develop into VT even when stimulated with the maximum PES strength (Figure 1G). At week 1 after MI when the scar tissue was still immature, the majority of WT and KO hearts only exhibited isolated or coupled PVCs with VT induced in only one WT heart (Figure 1G), suggesting a low inducibility of VT at this subacute phase.

β-catenin knockout reduces the prolongation of QRS duration and QT interval after myocardial infarction

Surface ECG recording in live animals showed no difference between sham-operated KO and WT mice in any of the parameters analyzed (QT interval, QRS duration, PR internal and RR internal, Figure 2). WT mice that received LAD ligation (MI) surgery exhibited prolonged QT interval (starting at week 1) and increased QRS duration (starting at week 3), but showed no changes in PR or RR intervals, suggesting that MI led to left ventricular remodeling without significantly affecting the function of the central conduction system (sinoatrial node and atrioventricular node). The MI-induced QT interval prolongation and QRS duration increases were attenuated in KO mice compared with WT mice (Figure 2), which is consistent with reduced VT susceptibility in KO mice.

β-catenin knockout attenuates chamber dilation and pump dysfunction after myocardial infarction

Echocardiography (Figure 3A) showed no difference between sham-operated KO and WT mice in LV chamber dimension (end diastolic volume, EDV, Figure 3B) or pump function (ejection fraction, EF, Figure 3C). Post-MI WT mice exhibited marked LV dilation (EDV=118.0±16.5 μl, n=14 vs. 42.0±2.5 μl, n=9 in sham WT at week 8, $p<0.01$, Figure 3B) and pump dysfunction (EF=21.6±3.3%, n=14 vs. 64.7±1.5%, n=9 in sham WT at week 8, $p<0.01$, Figure 3C), but LV posterior wall thickness (LVPWd) was not changed (p=0.7488 by ANOVA, Figure 3D). In post-MI KO mice, LV dilation (EDV=77.8±7.8μl, n=13 vs. 44.4±3.1 μl, n=10 in sham KO at 8-week, p=0.064, Figure 3B) and pump dysfunction (EF=34.9±4.3%, n=13 vs.

65.3±1.1%, n=10 in sham KO at 8-week, p<0.01, Figure 3C) were attenuated (p<0.01) compared with post-MI WT mice.

β-catenin knockout reduces scar sizes after myocardial infarction

Masson's trichrome staining of sham-operated hearts did not show any difference in gross morphology between KO and WT mice (Figure 4A). Consistent with observations in echocardiogram, post-MI WT hearts showed LV chamber dilation and wall thinning (Figure 4A). The scar size, as determined by the % fibrotic area of the LV wall, was smaller in post-MI KO (Scar size 38.5±3.9%, n=5 vs. 50.3±3.1%, n=6 in post-MI WT at 8-week, p<0.05, Figure 4B).

Both Wnt agonists and antagonists are upregulated after myocardial infarction

Wnt pathways are fine-tuned by the soluble Wnt ligands and Wnt inhibitors on the extracellular side of the plasma membrane, as well as the receptors and co-receptors on the plasma membrane (Figure 5A). Our qPCR analyses of gene transcripts showed that a variety of Wnt ligands, inhibitors and receptors are upregulated in the border zone and infarct region of the mouse hearts after MI (Figure 5 and 6).

Wnt ligands (agonists): Among the first group of Wnt ligands known to selectively activate the β-catenin pathway (canonical Wnt ligands, Figure 5B), *Wnt1* was increased by 3-7 fold after MI, *Wnt3a* was increased by 1-2 fold, but *Wnt8a* was not altered (p=0.76). Among the second group of Wnt ligands that selectively activate the β-catenin-independent pathways (non-canonical Wnt ligands, Figure 5C), *Wnt7* was markedly increased (by > 20 fold in the infarct at both Week 1 and 8; by 16-19 fold in border at week 1 which reduced to 3-4 fold at week 8), *Wnt11* was not altered by MI but in the infarct tissues at week 8 its level in KO was 57% less than in WT (p<0.05), and *Wnt5a* in KO sham hearts was 28% lower than in WT sham hearts and at week 8 after MI it was reduced by 17-41%. Among the third group of Wnt ligands that have been reported to activate both β-catenin dependent and independent pathways or have less defined functions (Figure 5D), three Wnt ligands (*Wnt4*, *Wnt10a* and *Wnt2*) were markedly increased at week1 (by 17-35 fold, 5-7 fold, and 2-4 fold respectively) but at week 8 they declined and, in the border zone, returned to the sham levels, while the other two Wnt ligands (*Wnt6* and *Wnt9a*) were only marginally increased (by 1.1-1.5 fold and 1.2-1.9 fold, respectively).

Wnt inhibitors (antagonists): Secreted frizzled-related proteins (Sfrp) are soluble Wnt inhibitors that prevent the binding between Wnt ligands and their plasma membrane receptors (frizzled).[31] At week 1 after MI, *Sfrp2* showed the largest increase (by 97-256 fold, Figure 5E), while the other two isoforms (*Sfrp3* and *Sfrp1*) also showed significant increases (by 16-32 fold, and 17-30 fold, respectively). At week 8, all three *Sfrp* levels have declined in border zone but remained high in the infarct region. Dickkopf-related proteins (Dkk) are another group of soluble Wnt inhibitors that selectively inhibit Wnt/β-catenin pathway by causing endocytosis of Wnt co-receptors (Lrp5/6) from the plasma membrane.[32] *Dkk3* was increased by 6-11 fold at week 1 and was further increased to 22-32 fold in the infarct at week 8 (Figure 5E). *Dkk1* was marginally increased (by 1.3-2.0 fold), while *Dkk4* was not affected by MI (p=0.801).

Wnt receptors and co-receptors: Frizzled (Fzd) proteins are seven-transmembrane proteins that serve at the receptors for Wnt ligands on the plasma membrane (Figure 5A). Among the 9 Fzd genes, the mostly affected by MI are *Fzd1*, *Fzd2* and *Fzd5* that were increased at week1 (by 5-7 fold, 8-13 fold, and 2-4 fold, respectively) but in the border zones at week 8 they all showed a significant decline. *Fzd7* and *Fzd9* had small or no increases at week 1 but were significantly increased in the infarct at week 8 (by 3-fold and 4-fold, respectively). Lipoprotein receptor-related protein 5 and 6 (Lrp5/6) are co-receptors required for Wnt ligand-induced activation of β-catenin pathway. As shown in Figure 6B, both *Lrp5* and *Lrp6* showed a small increase at week 1 (by 1.7-2.3 fold and 1.5-2.0 fold, respectively) but in the border zone at week 8 they both returned to the sham levels. *Ror2* and *Vangl2* are co-receptors required for non-canonical Wnt mediated activation of β-catenin-independent pathways. *Ror2* and *Vangl2* were increased at week 1 (by 4-9 fold and 2-4 fold, respectively) and they also showed a significant decline in border zone at week 8.

β-catenin protein: In cells not stimulated with Wnt/β-catenin pathway ligands, β-catenin in the cytoplasm is phosphorylated at Ser33/Ser37/Thr41 which labelling them for ubiquitination and degradation.[33] The level of β-catenin that is not phosphorylated at Ser33/Ser37/Thr41 (i.e., active β-catenin) is an index of the Wnt/β-catenin pathway activation in the cells.[34] As shown in Figure 6C, active β-catenin was increased in the border zone myocardium of WT hearts at 1 week after LAD ligation, suggesting activation of the Wnt/β-catenin pathway in the myocardium tissue (whole tissue lysate was used in the western blot studies). However, a similar increase in active β-catenin at 1 week was found in KO hearts in which only the cardiomyocytes were deleted of β-catenin. This suggests that the increase in active β-catenin at 1 week is primarily a result of activation of the Wnt/β-catenin pathway in non-cardiomyocytes (such as fibroblasts and inflammatory cells). In addition, the increased total β-catenin in KO hearts at 1 week also suggests increased proportion of non-cardiomyocytes (e.g., by fibroblast proliferation and infiltration of inflammatory cells) in the border zone myocardium. These observations suggest that the Wnt/β-catenin pathway is not activated in the cardiomyocytes of border zone myocardium in the subacute (1 week) and chronic (8 week) phases after myocardial infarction.

Ion channel gene expressions after myocardial infarction

Ion channels genes for ventricular depolarizing and repolarizing currents: In the border zone at week 1, the cardiac Na^+ channel gene transcript (*Scn5a,* encoding $Na_v1.5$) was reduced ($P<0.01$) by 46% and L-type Ca^{2+} channel gene (*Cacna1c*, encoding $Ca_v1.2$) was increased by 3.3 fold ($p<0.05$, Figure 7A). However, at week 8 both *Scn5a* and *Cacna1c* in the border zone have returned to near sham levels. In the infarct tissues, decreased *Scn5a* and increased *Cacna1c* were found at both week 1 and 8. All the major ventricular K^+ channel genes, including I_{to} (*Kcnd2, Kcnd3*), I_{Kr} (*Kcnh2*), I_{Ks} (*Kcnq1*) and I_{K1}(*Kcnj2*), were reduced in both border and infarct tissues at both week 1 and 8. However, no differences were seen between KO and WT groups in any of these ion channel genes except *Scn5a* which was significantly reduced in WT but not in KO in the border zone at Week 1.

Gap junctions and HCN channels: In the border zone, transcript of Cx43 (*Gja1*), the predominant gap junction isoform in ventricular myocardium, was reduced at week 1 but it returned to near sham levels at

week 8 (Figure 7B). However, immunostaining of Cx43 protein in border zones of both KO and WT hearts at week 8 showed that Cx43 is more diffusively distributed and is no longer restricted to cell-cell junction regions (intercalated disks) as seen in sham groups (Figure 7C). Cx40 (*Gja5*), which is expressed in the Purkinje fibers, was not affected by MI (Figure 7B). Among the genes of HCN channels that, if increased, will enhance myocyte automaticity, *Hcn1* was increased while *Hcn2* and *Hcn4* were reduced at week 1 but they returned to near sham levels at week 8 (Figure 7B). Again, no differences were seen between KO and WT hearts in these gene transcript levels.

Discussion

Although Wnt/β-catenin signaling has been studied in animal models of ischemic heart disease, this is the first study to investigate the post-MI arrhythmogenesis using β-catenin knockout mice. The reduced susceptibility to VT in β-catenin KO mice after MI is likely due to attenuated structural remodeling. The low VT inducibility at week-1 in both WT and KO mice when the scar was immature and at week-8 in KO mice that had a smaller scar highlights the importance of structural remodeling in VT induction. Previous studies in patients have also demonstrated a positive relationship between scar sizes and the risk for VT.[35] In addition, large scar sizes are associated with a longer cycle length for monomorphic VT,[36] further supporting the reentry as the predominant mechanism for VT in post-MI hearts.[37]

The increased QRS duration, reflecting electrical dyssynchrony, is commonly found in heart failure patients and has been demonstrated to be an independent predictor of mortality in these patients.[38,39] Consistent with this, in the present study the increased QRS in post-MI WT hearts is associated with a greater VT inducibility. The increased QRS in these mice are likely secondary to the structural remodeling (scar and chamber dilation), as well as possible reductions in the conduction velocity of Purkinje fibers (arborization block) which is common in ischemic heart failure.[40] The QT interval and its dispersion are positively associated with the scar size in patients with MI and their increases are a risk factor for VT.[41] The attenuated increases in both QRS duration and QT intervals in β-catenin KO mice are consistent with their reduced VT inducibility and a smaller scar size.

The different structural remodeling after MI between β-catenin KO and WT mice is unlikely due to differential activation of the Wnt/β-catenin pathway in cardiomyocytes at the subacute and chronic phases, because our results showed that the pathway was not activated in cardiomyocytes. While previous studies have reported conflicting results regarding the role of β-catenin in post-MI structural remodeling (as reviewed in the Introduction), our observations are consistent with the study by Zelarayan *et al.*, which also found a smaller scar size in β-catenin KO mice at 4 weeks after MI (LAD ligation).[29] The study by Zelarayan *et al.* also suggested that enhanced cardiac regeneration via activation of a cardiac progenitor population in the infarcted region may be a mechanism for the reduced scar in β-catenin KO hearts.[29] However, it remains to be determined if this enhanced regeneration in β-catenin KO hearts is due to attenuated activation of Wnt pathways in the acute phase after MI (within 7 days), as demonstrated by previous studies,[14] or is due to the Wnt-independent roles of β-catenin.[33]

Although we and others have previously demonstrated regulation of cardiac ion channel gene expression by Wnt/β-catenin signaling, ion channel alterations are unlikely playing a role in the different VT inducibilities between KO and WT hearts after MI. Although the in-depth mechanisms of arrhythmias were not studied using a mapping technique, our *ex vivo* ECG studies demonstrated similar frequency of isolated or coupled PVCs between WT and KO hearts after MI. This suggests that the VT-triggering mechanisms (i.e. triggered activity[10] or enhanced automaticity), are similarly developed in both groups. This is corroborated by the similar downregulations in K^+ channel genes and redistribution of Cx43 protein in both WT and KO hearts. In addition, it has been controversial about whether the cardiac Na^+ channel gene (*Scn5a*) expression is reduced after MI. The present study demonstrated that *Scn5a* transcript is reduced in the subacute phase (week 1) but not at the chronic phase (week 8) after MI. However, the high VT inducibility in WT mice at week 8, but not at week 1, highlights the critical role of a mature scar in VT induction. HCN channels have been shown to play a role in the arrhythmogenesis of dilated cardiomyopathy, and HCN2-overexpressing hearts have increased VT susceptibility.[42] In the present study, the selective upregulation of *Hcn1* gene is consistent with previous studies using a mouse model of cardiac hypertrophy, although *Hcn2* and *Hcn4* are more abundant than *Hcn1*.[43]

In summary, this study demonstrated that inhibition of β-catenin reduces ventricular tachyarrhythmias in post-MI hearts due to attenuated structural remodeling, but without affecting ion channel gene alterations. Because the Wnt/β-catenin pathway is not activated in cardiomyocytes of post-MI hearts at both the subacute and chronic phases, the effect of β-catenin on VT is likely mediated by its Wnt-independent roles. In addition, this study only examined the ischemic heart failure mouse model, and future studies are warranted to investigate the Wnt/β-catenin pathway activation in cardiomyocytes and its role in arrhythmogenesis in other types of heart failure, such as the pressure-overload induced heart failure.

Methods

All procedures were approved by the institutional animal care committee at the University of Ottawa (Protocol #: HI-2602), and were performed in accordance with relevant guidelines and regulations. All the studies involving live animals were reported as described by the ARRIVE guidelines.[44]

Mice

To generate cardiomyocyte-specific β-catenin (*Ctnnb1*) knockout mice, *Ctnnb1*$^{flox/flox}$ mice (with exons 2 to 6 floxed, Jackson Lab, Stock No: 004152) were crossbred with αMHC-MerCreMer mice (Jackson Lab, Stock No: 005650) to obtain *Ctnnb1*$^{flox/flox}$;αMHC-MerCreMer$^{+/-}$ mice (Figure 1A). Littermate *Ctnnb1*$^{flox/flox}$;αMHC-MerCreMer$^{-/-}$ mice were used as control wild-type mice. At the age of 8-12 weeks, all mice received daily subcutaneous injection of tamoxifen (20 mg/kg, Sigma, Catalogue No.:T5648, dissolved in sunflower seed oil at 10 mg/ml) for 5 consecutive days (Figure 1B). At 7 days after the last tamoxifen injection, baseline surface ECG and echocardiogram were recorded before the experimental

myocardial infarction surgery as described below. Both male and female mice were used to investigate any sex-specific effects. A total of 45 WT mice (20 male and 25 female) and 40 KO mice (20 male and 20 female) were used in this study.

Experimental Myocardial Infarction

Myocardial infarction was induced in mice by permanent ligation of the left anterior descending (LAD) coronary artery as we previously described.[45] Mice were injected with buprenorphine (0.05 mg/kg; subcutaneous) 1 hour prior to surgery and twice daily thereafter for 3 days. During the surgery, mice were incubated, anesthetized using 2% isoflurane and maintained under physiologic temperature control. The heart was exposed after a left thoracotomy, the LAD was identified under a dissection microscope (Topcon Corporation, Model No.: OMS-75) and ligated at 0.3 mm distal to the atrioventricular junction using a Prolene 7.0 suture. Successful LAD ligation was confirmed by the pale color of the affected myocardium before chest closure with a Prolene 6.0 suture.

Surface ECG and Echocardiography

ECG with limb Lead I and II were recorded in mice at one day before and at week 1, 3, 5 and 8 after the LAD ligation using ADInstruments small animal ECG system (Powerlab 8/35 and Animal Bio Amp) and data were analyzed using LabChart 8.0. During ECG recording, mice were anesthetized with 1.5-2.0% isoflurane and body temperature were kept at 37°C using a heating pad. Echocardiography was recorded using a VEVO3100 system with the MS400 transducer (VisualSonic Inc., Toronto), and images were analyzed in VevoLab software. During recording, animals were anaesthetized under 1.5-2% isoflurane with body temperature maintained at 37°C using a heating pad. To minimize the influence of heart rate on pump function, echocardiogram was recorded when heart rates were in the 400-500 bpm range. M-mode tracing of the left ventricle (LV) was recorded in the short-axis view at the mid-papillary level. Three consecutive cardiac cycles, measured in VevoLab, were averaged to determine ejection fraction % (EF), fractional shortening % (FS), end-diastolic volume (EDV), end-systolic volume (ESV), left ventricular internal diameter (LVIDs/LVIDd), and posterior wall thickness. The EF was calculated using the following equation: $(LVIDd^3 – LVIDs^3)/LVIDd^3 \times 100$. FS was calculated using the following equation: (LVIDd–LVIDs)/LVIDd×100. B-mode tracing of the LV was recorded in the parasternal long-axis view and analyzed using the LV trace function in VevoLab to determine EF, FS, EDV, ESV, and LV volume.

Programmed electrical stimulation (PES) in isolated mouse hearts

At 1 and 8 weeks after MI, mouse hearts were isolated and Langendorff-perfused with Tyrode solution (37°C) containing 1 μM isoproterenol (Sigma, Catalogue No.: I6504), *ex vivo* ECG were continuously measured by placing recording electrodes around the heart as we previously described[20,46] (Figure 1E). PES was applied using a MyoPacer (IonOptix) via a pair of platinum electrodes placed on the left ventricular apex of the heart. The standard stimulation protocol (Figure 1E) consisted of 10 stimuli at 100 ms intervals (S1, 5V) followed by one extra stimulus (S2) starting at an interval of 80 ms which was then reduced by 2 ms until the effective refractory period (ERP) was reached. If VT or VF was not induced, a

second extra stimulus (S3) was added at 80 ms after S2. The S3 interval was then reduced by 2 ms until the ERP was reached. Finally, a third extra stimulus (S4) was added 80 ms after S3 and was then decreased by 2 ms until the ERP was reached. If a heart failed to develop a VT or VF with 3 extra stimuli, the heart was deemed non-inducible.

Masson's Trichrome staining

Mouse hearts were fixed by retrograde perfusion via the aorta with 4% paraformaldehyde (diluted in PBS) for 10 min at room temperature. The hearts were then incubated in increasing concentrations of sucrose dissolved in PBS (10% for overnight, 20% for 8 h, and 30% for overnight) on a horizontal rotator at 4°C before being embedded in TissueTek OCT compound. Hearts were then cryosectioned at 10-μm slices using a Leica vibrating microtome (Model No.: CM3050S) at five different levels of the heart from the ligation site to the apex at 300-μm intervals. Ten consecutive slices were made for each level. Heart sections were then stained using a Masson's Trichrome Staining kit (Sigma, Catalogue No.: HT15) according to the manufacturer's instructions. Fibrosis areas were analyzed with ImageJ software using the Colour Deconvolution for Masson's Trichrome Stain tool. The scar size for each the 5 different levels was calculated as the percentage of fibrotic area to the total area of the left ventricle section. The heart's total scar size was then calculated as the mean of the scar sizes at the 5 levels and reported in Figure 4.

Immunohistostaining

Cryosectioned heart slices, as prepared above, were blocked and permeabilized in Dako protein block (Agilent, Catalogue No.: X0909) containing 0.1% (w/v) saponin (Sigma, Catalogue No.: 47036) at room temperature for 90 min. Slices were incubated with primary antibodies (see below) diluted in the same blocking solution at 4°C for overnight. After washing with PBS, slices were incubated with secondary antibodies (see below) at room temperature for 1 h. After washing with PBS for three times, slices were mounted with ProLong gold antifade reagent containing DAPI (ThermoFisher, Catalogue No.: P36931). Primary antibodies used were polycloncal rabbit anti-Cx43 (1:200, Sigma, Catalogue No.: C6219), and monoclonal mouse anti-α-sarcomeric actinin (1:400, Sigma, Catalogue No.: A7811). Secondary antibodies used were anti-rabbit IgG (Alexa Fluor-488, 1:300) and anti-mouse IgG (Alexa Fluor-568, 1:300). Fluorescent images of the myocardium of left ventricular free wall of sham hearts and border zone of MI-hearts were taken with a ZEISS confocal microscope equipped with the Airyscan technique for high-resolution imaging (Zeiss Elyra S.1 LSM 880).

Real-Time Quantitative PCR (qPCR)

Total RNA was isolated from the border zone and infarct region of mouse hearts with Trizol reagent (ThermoFisher, Catalogue No.: 15596026) and digested with Turbo DNA-*free* kit (ThermoFisher, Catalogue No.: AM1907) to remove genomic DNA, according to manufacturer's instruction. One μg RNA was used for cDNA synthesis with a High-Capacity cDNA Reverse Transcription Kit (ThermoFisher, Catalogue No.: 4368814). Real-time quantitative PCR was performed on a CFX Connect Real-Time PCR Detection System (Bio-Rad) using standard SYBR green method. Information of the qPCR primers was included in the Table

in the Online Supplement. No reverse transcriptase (RT-) controls and no template controls (NTC) were included for all the primers to make sure that there were no genomic DNA contamination or primer dimer signals. Transcript level of target genes was normalized to the level of *Hprt1* mRNA in the same sample. Results were analyzed with the $2^{-\Delta\Delta C(t)}$ method.

Western Blotting

The border zone myocardium tissue of the post-LAD ligation hearts (week 1 and 8) or the left ventricular anterior free wall of sham-operated hearts were homogenized in T-PER Tissue Protein Extraction Reagent (ThermoFisher, 78510) containing Halt Protease Inhibitor Cocktail (ThermoFisher, 87786). Protein concentration was determined using Pierce Rapid Gold BCA Protein Assay Kit (ThermoFisher, A53226) and cell lysates (10 µg protein per lane) were run on a 4-12% SDS-polyacrylamide gel and transferred onto a PVDF membrane. The transferred membrane was incubated with a primary antibody (see below) overnight at 4°C, followed by a 2-h incubation with a peroxidase-conjugated secondary antibody (1:2000, Cell Signaling, #7074). Primary antibodies used were rabbit anti-non-phospho (active) β-Catenin (Ser33/Ser37/Thr41) (1:1000, Cell signaling, #8814) and rabbit anti-total β-Catenin (1:1000, Cell signaling, #8480). Immunoreactivity was detected by chemiluminescence (Pierce™ ECL Western Blotting Substrate, ThermoFisher, 32209). Equal protein loading of the gels was assessed by re-probing the membrane with rabbit anti-GAPDH antibody (1:2000, Cell Signaling, #2118). Band densities were quantified using the “Gel Analyzer Protocol” function of ImageJ (https://imagej.nih.gov/ij/docs/menus/analyze.html#gels), and presented as values after normalization to GAPDH in the same samples. All the original uncropped gel images are included in Supplementary Figure 1.

Statistical Analysis

Statistical analysis adhered to the Journal Guidelines. Data are expressed as mean ± SEM with $p<0.05$ considered significant. Sample number indicates the number of biological replicates (each individual mouse is considered one sample). Differences between two means were evaluated by two-tailed Student’s *t*-test. Differences among multiple means were assessed by one-way or two-way analysis of variance (ANOVA). When significance was detected by ANOVA, differences among individual means were evaluated *post hoc* by Bonferroni’s test.

Declarations

Acknowledgements

This work was supported by the Canadian Institutes of Health Research (Grant number: PJT-148918, to W.L.), and McDonald Scholarship and New Investigator Award from Heart and Stroke Foundation of Canada (Grant number: S-17-LI-0866, to W.L.).

Author contributions

J.W. and W.L conceived the experiments. J.W., Y.X., A.L., and H.W. performed experiments. J.W., D.R.D., P.L., R.S.B. and W.L. analyzed and interpreted results and wrote the manuscript. All authors reviewed and approved the manuscript.

Additional information

The authors declare that there is no competing interest.

References

1 Benjamin, E. J. *et al.* Heart Disease and Stroke Statistics-2018 Update: A Report From the American Heart Association. *Circulation***137**, e67-e492, doi:10.1161/cir.0000000000000558 (2018).

2 Chugh, S. S. Sudden cardiac death in 2017: Spotlight on prediction and prevention. *Int J Cardiol***237**, 2-5, doi:10.1016/j.ijcard.2017.03.086 (2017).

3 Zheng, Z. J., Croft, J. B., Giles, W. H. & Mensah, G. A. Sudden cardiac death in the United States, 1989 to 1998. *Circulation***104**, 2158-2163 (2001).

4 Roy, D. *et al.* Long-term reproducibility and significance of provokable ventricular arrhythmias after myocardial infarction. *J Am Coll Cardiol***8**, 32-39 (1986).

5 Marchlinski, F. E., Waxman, H. L., Buxton, A. E. & Josephson, M. E. Sustained ventricular tachyarrhythmias during the early postinfarction period: electrophysiologic findings and prognosis for survival. *J Am Coll Cardiol***2**, 240-250 (1983).

6 Jackson, N., Gizurarson, S., Massé, S. & Nanthakumar, K. in *Cardiac Electrophysiology: From Cell to Bedside, 2018* (eds D. P. Zipes, J. Jalife, & W. G. Stevenson) Ch. 48.

7 Tomaselli, G. F. & Zipes, D. P. What causes sudden death in heart failure? *Circ Res***95**, 754-763, doi:10.1161/01.RES.0000145047.14691.db (2004).

8 Pu, J. & Boyden, P. A. Alterations of Na+ currents in myocytes from epicardial border zone of the infarcted heart. A possible ionic mechanism for reduced excitability and postrepolarization refractoriness. *Circ Res***81**, 110-119 (1997).

9 Wit, A. L. & Peters, N. S. The role of gap junctions in the arrhythmias of ischemia and infarction. *Heart Rhythm***9**, 308-311, doi:10.1016/j.hrthm.2011.09.056 (2012).

10 Gilmour, R. F., Jr., Heger, J. J., Prystowsky, E. N. & Zipes, D. P. Cellular electrophysiologic abnormalities of diseased human ventricular myocardium. *The American journal of cardiology***51**, 137-144, doi:10.1016/s0002-9149(83)80024-1 (1983).

11 Gessert, S. & Kühl, M. The multiple phases and faces of wnt signaling during cardiac differentiation and development. *Circ Res***107**, 186-199, doi:10.1161/circresaha.110.221531 (2010).

12 Liang, W. *et al.* Canonical Wnt signaling promotes pacemaker cell specification of cardiac mesodermal cells derived from mouse and human embryonic stem cells. *Stem Cells***38**, 352-368, doi:10.1002/stem.3106 (2020).

13 Hou, N. *et al.* Transcription Factor 7-like 2 Mediates Canonical Wnt/beta-Catenin Signaling and c-Myc Upregulation in Heart Failure. *Circ Heart Fail***9:e003010**, doi:10.1161/CIRCHEARTFAILURE.116.003010 e003010

10.1161/circheartfailure.116.003010 (2016).

14 Duan, J. *et al.* Wnt1/betacatenin injury response activates the epicardium and cardiac fibroblasts to promote cardiac repair. *Embo J***31**, 429-442, doi:10.1038/emboj.2011.418 (2012).

15 Dawson, K., Aflaki, M. & Nattel, S. Role of the Wnt-Frizzled system in cardiac pathophysiology: a rapidly developing, poorly understood area with enormous potential. *J Physiol***591**, 1409-1432, doi:10.1113/jphysiol.2012.235382 (2013).

16 Iyer, L. M. *et al.* A context-specific cardiac β-catenin and GATA4 interaction influences TCF7L2 occupancy and remodels chromatin driving disease progression in the adult heart. *Nucleic Acids Res***46**, 2850-2867, doi:10.1093/nar/gky049 (2018).

17 Malekar, P. *et al.* Wnt signaling is critical for maladaptive cardiac hypertrophy and accelerates myocardial remodeling. *Hypertension***55**, 939-945, doi:10.1161/HYPERTENSIONAHA.109.141127 (2010).

18 Borrell-Pages, M. *et al.* LRP5/canonical Wnt signalling and healing of ischemic myocardium. *Basic Res Cardiol***111**, 67, doi:10.1007/s00395-016-0585-y (2016).

19 Liang, W., Cho, H. C. & Marban, E. Wnt signalling suppresses voltage-dependent Na(+) channel expression in postnatal rat cardiomyocytes. *J Physiol***593**, 1147-1157 (2015).

20 Lu, A. *et al.* Direct and indirect suppression of Scn5a gene expression mediates cardiac Na+ channel inhibition by Wnt signalling. *Can J Cardiol***36**, 564-576, doi:https://doi.org/10.1016/j.cjca.2019.09.019 (2020).

21 Wang, N. *et al.* Activation of Wnt/beta-catenin signaling by hydrogen peroxide transcriptionally inhibits NaV1.5 expression. *Free Radic Biol Med***96**, 34-44, doi:10.1016/j.freeradbiomed.2016.04.003 (2016).

22 Zhao, L., Sun, L., Lu, Y., Li, F. & Xu, H. A small-molecule LF3 abrogates beta-catenin/TCF4-mediated suppression of NaV1.5 expression in HL-1 cardiomyocytes. *J Mol Cell Cardiol***135**, 90-96, doi:10.1016/j.yjmcc.2019.08.007 (2019).

23 Gillers, B. S. *et al.* Canonical wnt signaling regulates atrioventricular junction programming and electrophysiological properties. *Circ Res***116**, 398-406, doi:10.1161/CIRCRESAHA.116.304731 (2015).

24 Li, G. *et al.* Differential Wnt-mediated programming and arrhythmogenesis in right versus left ventricles. *J Mol Cell Cardiol***123**, 92-107, doi:10.1016/j.yjmcc.2018.09.002 (2018).

25 Ai, Z., Fischer, A., Spray, D. C., Brown, A. M. & Fishman, G. I. Wnt-1 regulation of connexin43 in cardiac myocytes. *J Clin Invest***105**, 161-171, doi:10.1172/JCI7798 (2000).

26 Hahn, J. Y. *et al.* Beta-catenin overexpression reduces myocardial infarct size through differential effects on cardiomyocytes and cardiac fibroblasts. *J Biol Chem***281**, 30979-30989, doi:10.1074/jbc.M603916200 (2006).

27 Oikonomopoulos, A. *et al.* Wnt signaling exerts an antiproliferative effect on adult cardiac progenitor cells through IGFBP3. *Circ Res***109**, 1363-1374, doi:10.1161/circresaha.111.250282 (2011).

28 Barandon, L. *et al.* Reduction of infarct size and prevention of cardiac rupture in transgenic mice overexpressing FrzA. *Circulation***108**, 2282-2289, doi:10.1161/01.cir.0000093186.22847.4c (2003).

29 Zelarayán, L. C. *et al.* Beta-Catenin downregulation attenuates ischemic cardiac remodeling through enhanced resident precursor cell differentiation. *Proc Natl Acad Sci U S A***105**, 19762-19767, doi:10.1073/pnas.0808393105 (2008).

30 Gharibeh, L. *et al.* GATA6 is a regulator of sinus node development and heart rhythm. *Proc Natl Acad Sci U S A***118**, doi:10.1073/pnas.2007322118 (2021).

31 Cruciat, C. M. & Niehrs, C. Secreted and transmembrane wnt inhibitors and activators. *Cold Spring Harbor perspectives in biology***5**, a015081, doi:10.1101/cshperspect.a015081 (2013).

32 Bao, J., Zheng, J. J. & Wu, D. The structural basis of DKK-mediated inhibition of Wnt/LRP signaling. *Science signaling***5**, pe22, doi:10.1126/scisignal.2003028 (2012).

33 Valenta, T., Hausmann, G. & Basler, K. The many faces and functions of beta-catenin. *Embo J***31**, 2714-2736, doi:10.1038/emboj.2012.150 (2012).

34 Wang, Z. *et al.* Wnt signaling activates MFSD2A to suppress vascular endothelial transcytosis and maintain blood-retinal barrier. *Sci Adv***6**, eaba7457, doi:10.1126/sciadv.aba7457 (2020).

35 Pride, Y. B. *et al.* Relation between myocardial infarct size and ventricular tachyarrhythmia among patients with preserved left ventricular ejection fraction following fibrinolytic therapy for ST-segment elevation myocardial infarction. *The American journal of cardiology***104**, 475-479, doi:10.1016/j.amjcard.2009.04.005 (2009).

36 Alexandre, J. *et al.* Scar extent as a predictive factor of ventricular tachycardia cycle length after myocardial infarction: implications for implantable cardioverter-defibrillator programming optimization. *Europace***16**, 220-226, doi:10.1093/europace/eut289 (2014).

37 Josephson, M. E., Horowitz, L. N. & Farshidi, A. Continuous local electrical activity. A mechanism of recurrent ventricular tachycardia. *Circulation***57**, 659-665, doi:10.1161/01.cir.57.4.659 (1978).

38 Wang, N. C. *et al.* Clinical implications of QRS duration in patients hospitalized with worsening heart failure and reduced left ventricular ejection fraction. *Jama***299**, 2656-2666, doi:10.1001/jama.299.22.2656 (2008).

39 Dhingra, R. *et al.* Electrocardiographic QRS duration and the risk of congestive heart failure: the Framingham Heart Study. *Hypertension***47**, 861-867, doi:10.1161/01.hyp.0000217141.20163.23 (2006).

40 He, B. J., Boyden, P. & Scheinman, M. Ventricular arrhythmias involving the His-Purkinje system in the structurally abnormal heart. *Pacing and clinical electrophysiology : PACE***41**, 1051-1059, doi:10.1111/pace.13465 (2018).

41 Puljevic, D., Smalcelj, A., Durakovic, Z. & Goldner, V. Effects of postmyocardial infarction scar size, cardiac function, and severity of coronary artery disease on QT interval dispersion as a risk factor for complex ventricular arrhythmia. *Pacing and clinical electrophysiology : PACE***21**, 1508-1516, doi:10.1111/j.1540-8159.1998.tb00237.x (1998).

42 Kuwabara, Y. *et al.* Increased expression of HCN channels in the ventricular myocardium contributes to enhanced arrhythmicity in mouse failing hearts. *J Am Heart Assoc***2**, e000150, doi:10.1161/jaha.113.000150 (2013).

43 Hofmann, F. *et al.* Ventricular HCN channels decrease the repolarization reserve in the hypertrophic heart. *Cardiovasc Res***95**, 317-326, doi:10.1093/cvr/cvs184 (2012).

44 Percie du Sert, N. *et al.* The ARRIVE guidelines 2.0: Updated guidelines for reporting animal research. *Br J Pharmacol***177**, 3617-3624, doi:10.1111/bph.15193 (2020).

45 Molgat, A. S. *et al.* Hyperglycemia inhibits cardiac stem cell-mediated cardiac repair and angiogenic capacity. *Circulation***130**, S70-76, doi:10.1161/circulationaha.113.007908 (2014).

46 Kapoor, N., Liang, W., Marban, E. & Cho, H. C. Direct conversion of quiescent cardiomyocytes to pacemaker cells by expression of Tbx18. *Nat Biotechnol***31**, 54-62, doi:10.1038/nbt.2465 (2013).

Figures

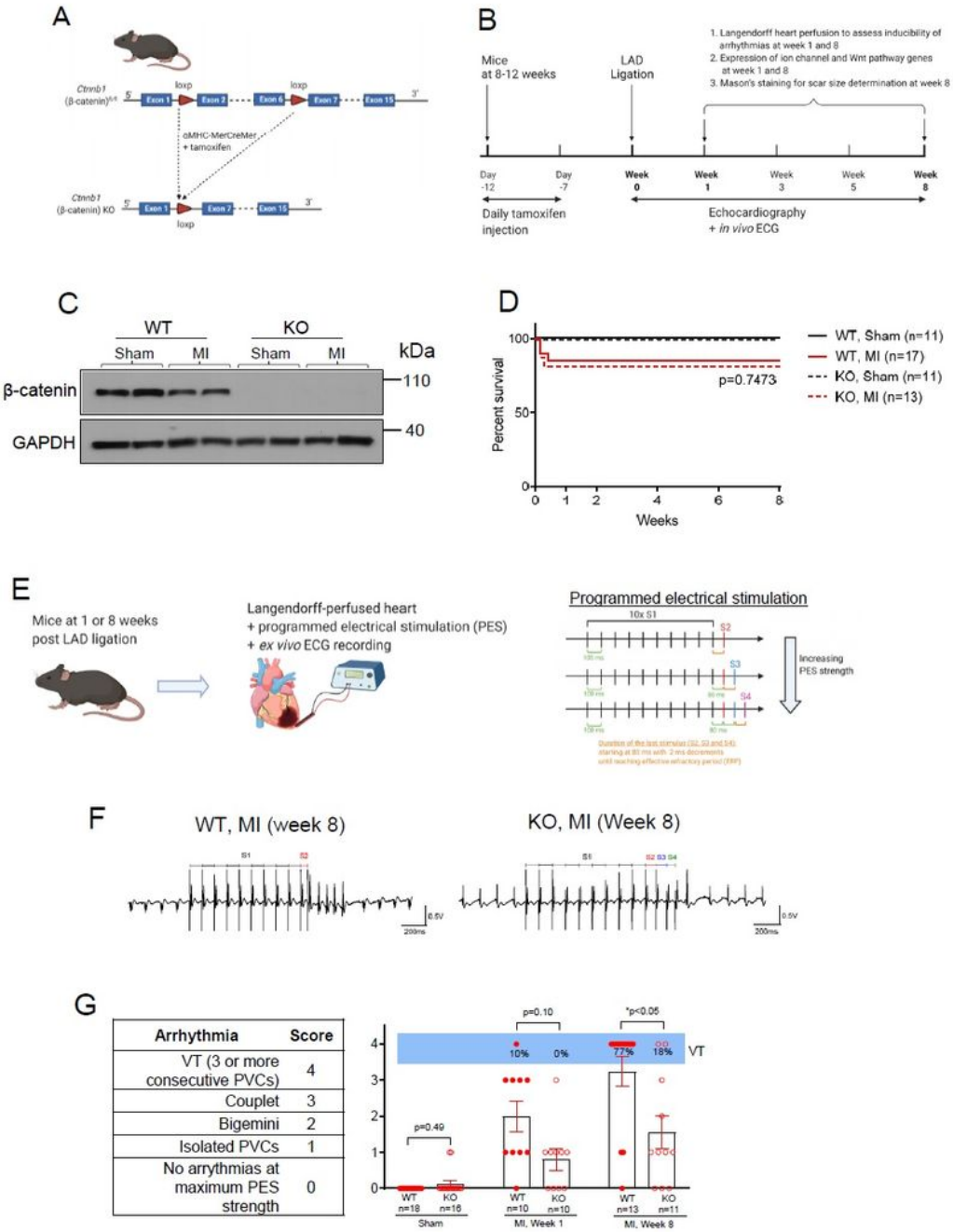

Figure 1

β-catenin knockout reduces the susceptibility to ventricular tachycardias after myocardial infarction. A. To generate cardiomyocyte-specific β-catenin (Ctnnb1) knockout mice, Ctnnb1flox/flox mice (with exons 2 to 6 floxed) were crossbred with αMHC-MerCreMer mice to obtain Ctnnb1flox/flox;αMHC-MerCreMer+/- mice, which were then treated with tamoxifen for deletion of exons 2-6 generating Ctnnb1 null allele due to the loss of the translational start site. Littermate Ctnnb1flox/flox;αMHC-MerCreMer-/- mice were used

as control wild-type mice. B. Experimental design. C. Representative western blot for confirmation of reduced total β-catenin in both sham and LAD-ligated (MI) KO hearts. Protein samples were prepared from left ventricular free wall of sham mice and from the border zone in mice at 8-weeks post-MI (myocardial infarction). GAPDH was used as a loading control. The original uncropped gel images are included in Supplementary Figure 1. D. Survival curve showing no difference in survival between WT and KO mice after LAD ligation (p=0.7473, analyzed by Log-rank (Mantel-Cox) test). Only the mice in the long-term (8-weeks after MI) study were included in this survival analysis. All mortality occurred within the first week. E. Protocols for evaluation of the inducibility of ventricular tachyarrhythmias (VT). Left Panel: Mouse hearts were isolated and Langendorff-perfused with Tyrode solution containing isoproterenol, ex vivo ECG were continuously measured by placing recording electrodes around the heart as we previously described.20,46 Programmed electrical stimulation (PES) was applied using a MyoPacer (IonOptix) via a pair of platinum electrodes placed on the left ventricular apex of the heart. Right Panel: the standard stimulation protocol consisted of 10 stimuli at 100 ms intervals (S1, 5V) followed by one extra stimulus (S2) starting at an interval of 80 ms which was then reduced by 2 ms until the effective refractory period (ERP) was reached. If VT or VF was not induced, a second extra stimulus (S3) was added at 80 ms after S2. The S3 interval was then reduced by 2 ms until the ERP was reached. Finally, a third extra stimulus (S4) was added 80 ms after S3 and was then decreased by 2 ms until the ERP was reached. If a heart failed to develop a VT or VF with 3 extra stimuli, the heart was deemed non-inducible. F. Representative ex vivo ECG (Lead II) showing PES-induced ventricular tachycardia (defined as 3 or more consecutive PVCs) in a WT heart (8-week after MI) when stimulated with one extra stimulus (S2), and only one single PVC in a KO heart (8-week after MI) when stimulated with three extra stimuluses (S4). G. Summary of PES-induced PVCs and VTs in WT and KO hearts at 1 or 8 weeks after MI. An arrhythmia score was assigned to each heart according to the criteria shown in the left table. At 8 weeks after MI, VT was successfully induced in 77% of WT hearts but only in 18% of KO hearts. Data were analyzed by two-way ANOVA and Bonferroni post-hoc comparison.

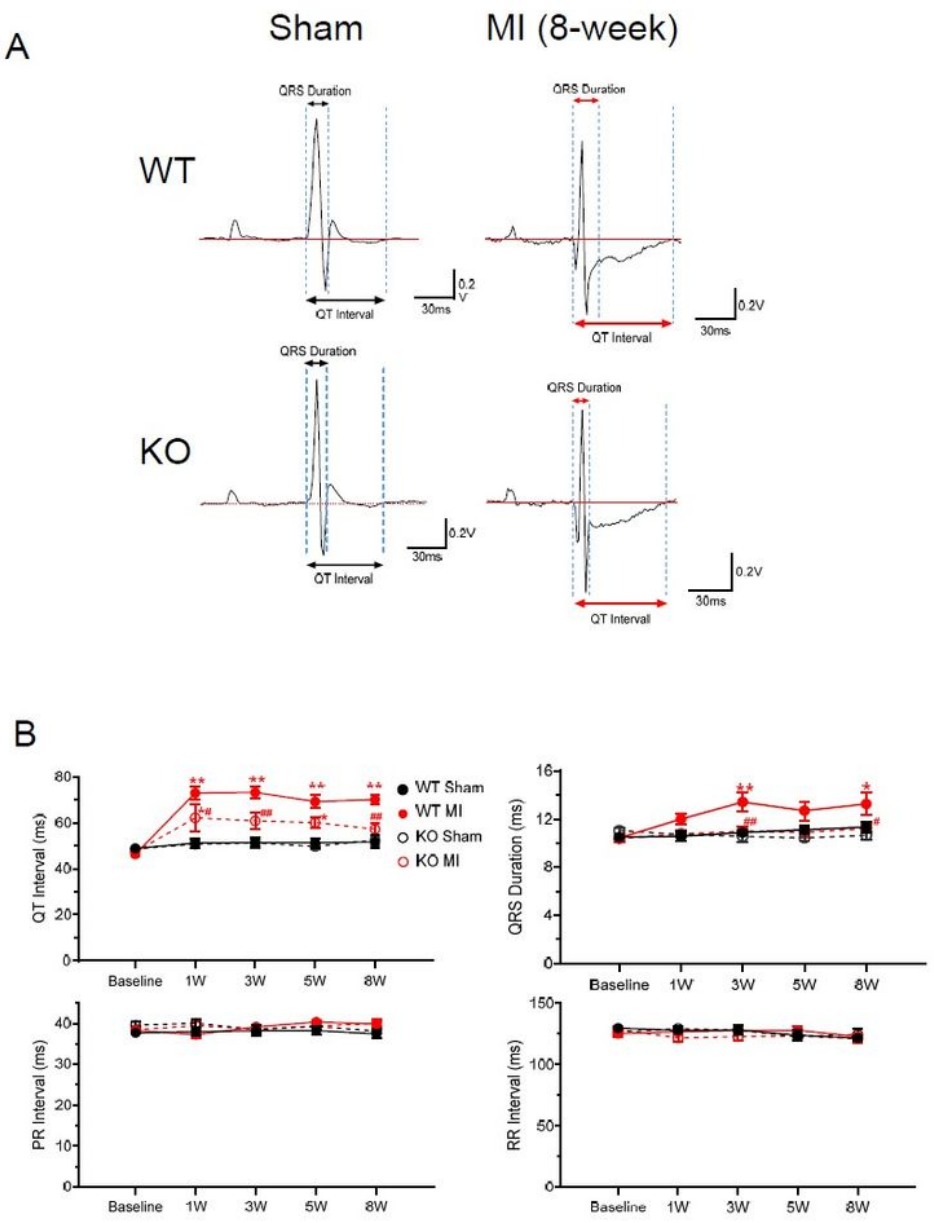

Figure 2

β-catenin knockout reduces the prolongation of QRS duration and QT interval after myocardial infarction. A. Representative in vivo surface ECG traces (Lead II) in sham mice (left) and in mice at 8 weeks after MI (right). B. Summary of in vivo ECG parameters, including QT Interval (top left), QRS duration (top right), PR Interval (bottom left), and RR Interval (bottom right). n=10-13 per group. *p<0.05, **p<0.01, vs.

corresponding sham groups; #p<0.05, ##p<0.01, vs. WT MI group at the indicated timepoints. Data were analyzed by two-way ANOVA and Bonferroni post-hoc comparison.

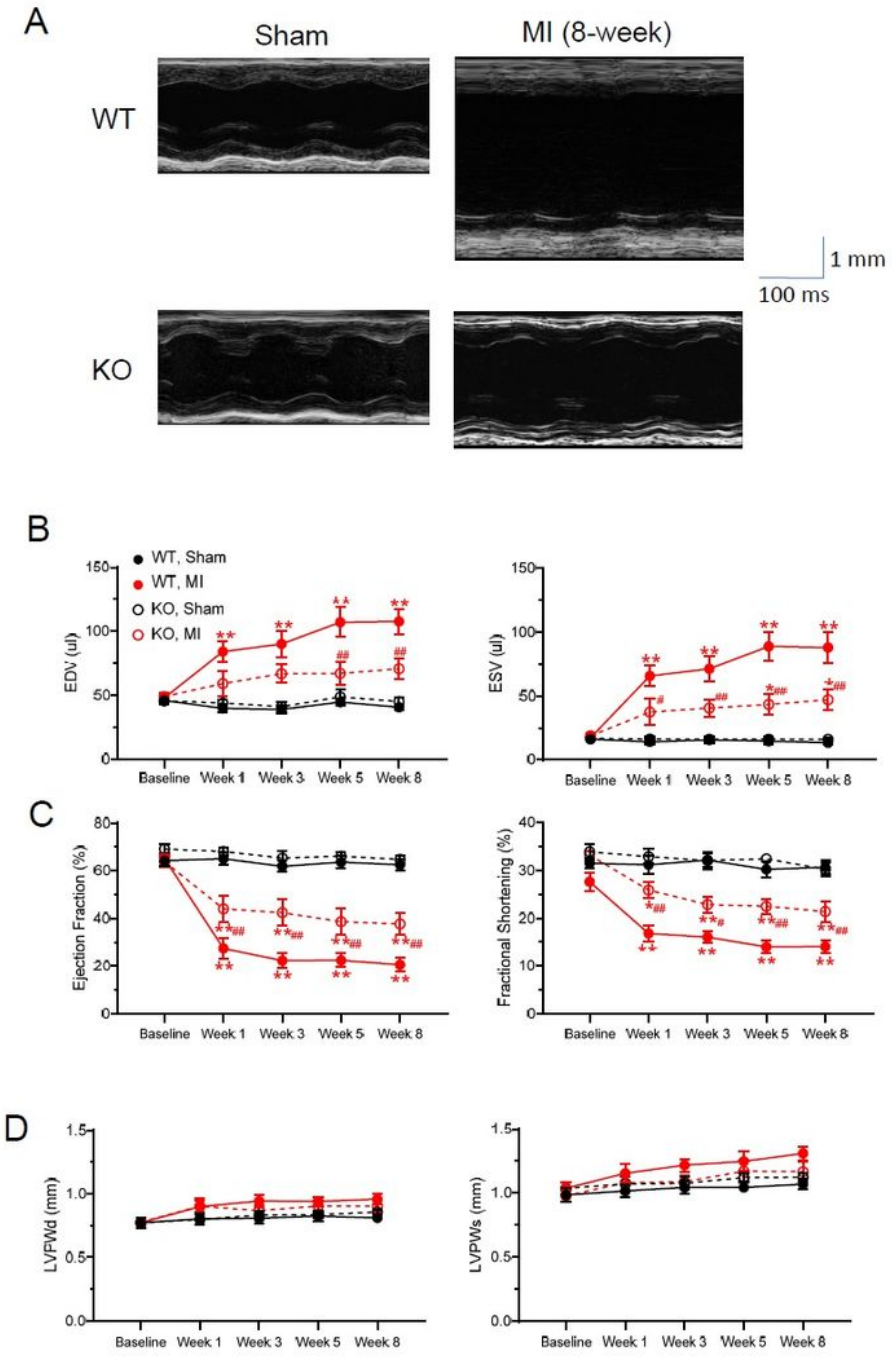

Figure 3

β-catenin knockout attenuates pump dysfunction and chamber dilation after myocardial infarction. A. Representative short axis, M-mode echocardiographic recordings at the left ventricular mid-papillary level showing attenuation of cardiac function and dilation in β-catenin KO mice post-MI. Echocardiogram was

recorded when heart rates were in the 400-500 bpm range. B to D. Summary of echocardiographic parameters of mice up to 8 weeks after MI showing reduced left ventricular dilation in KO mice as measured by end diastolic volume (EDV, panel B, left) and end systolic volume (ESV, panel B, right), attenuation of cardiac systolic dysfunction in KO mice as measured by ejection fraction (panel C, left) and fractional shortening (panel C, right), and unchanged left ventricular posterior wall thickness at diastole (LVPWd, panel D, left) and at systole (LVPDs, panel D, right). n=10-13 per group. *p<0.05, **p<0.01, vs. corresponding sham groups; #p<0.05, ##p<0.01, vs. WT MI group at the indicated timepoints. Data were analyzed by two-way ANOVA and Bonferroni post-hoc comparison.

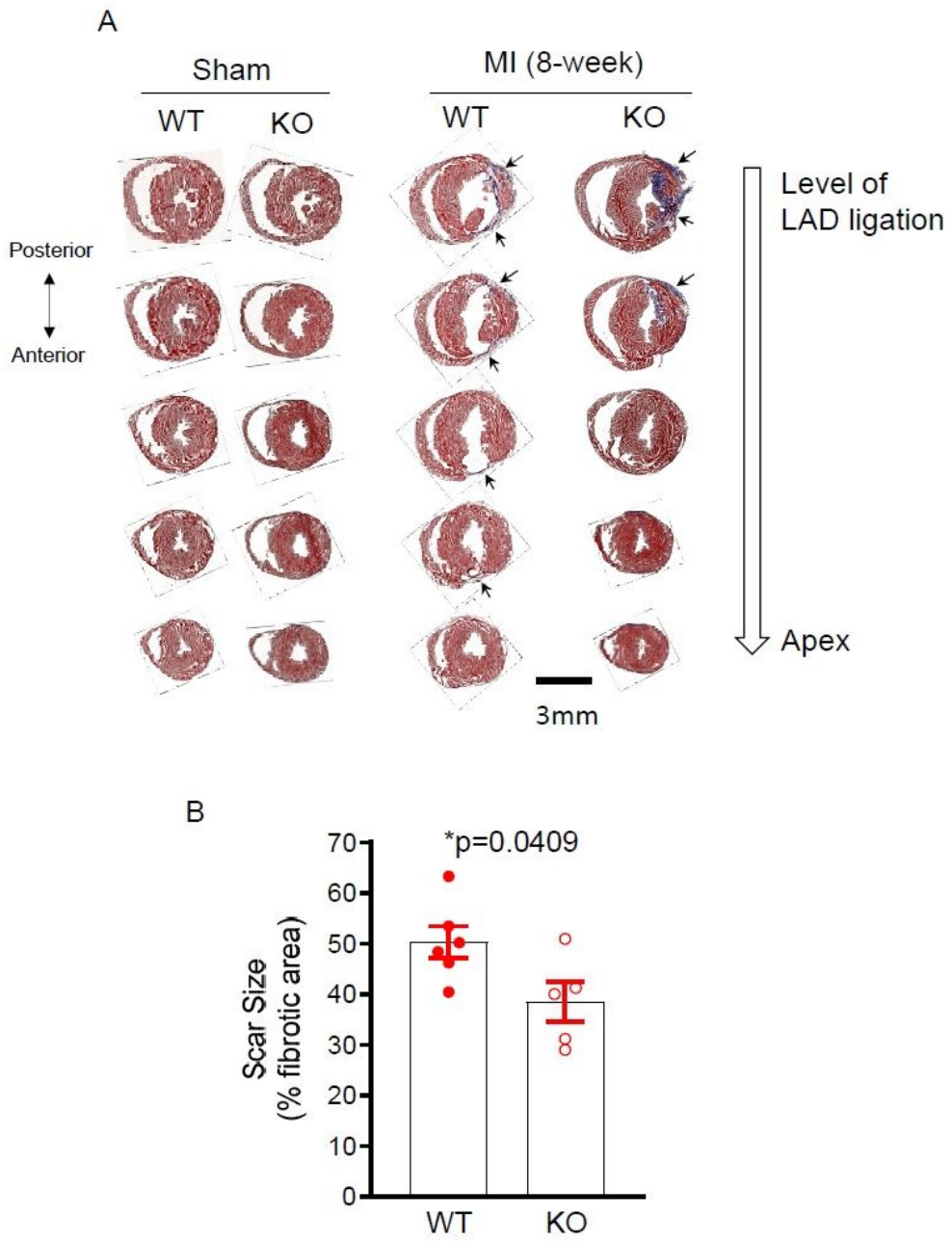

Figure 4

β-catenin knockout reduces scar sizes after myocardial infarction. A. Representative images of Masson's trichrome staining of mouse heart tissue sections at 5 different levels from LAD ligation site (top) to the apex (bottom) at 8 weeks after MI (right), as well as in sham-operated hearts (left). The scar size for each the 5 different levels was calculated as the percentage of fibrotic area (as indicated by the arrows) to the total area of the left ventricle section. The heart's total scar size was then calculated as the mean of the

scar sizes at the 5 levels and reported in panel B. B. Summary of scar size showing reduced scar size in KO hearts (n=5) compared to WT hearts (n=6). Statistical analysis was performed with a two-tailed unpaired t-test.

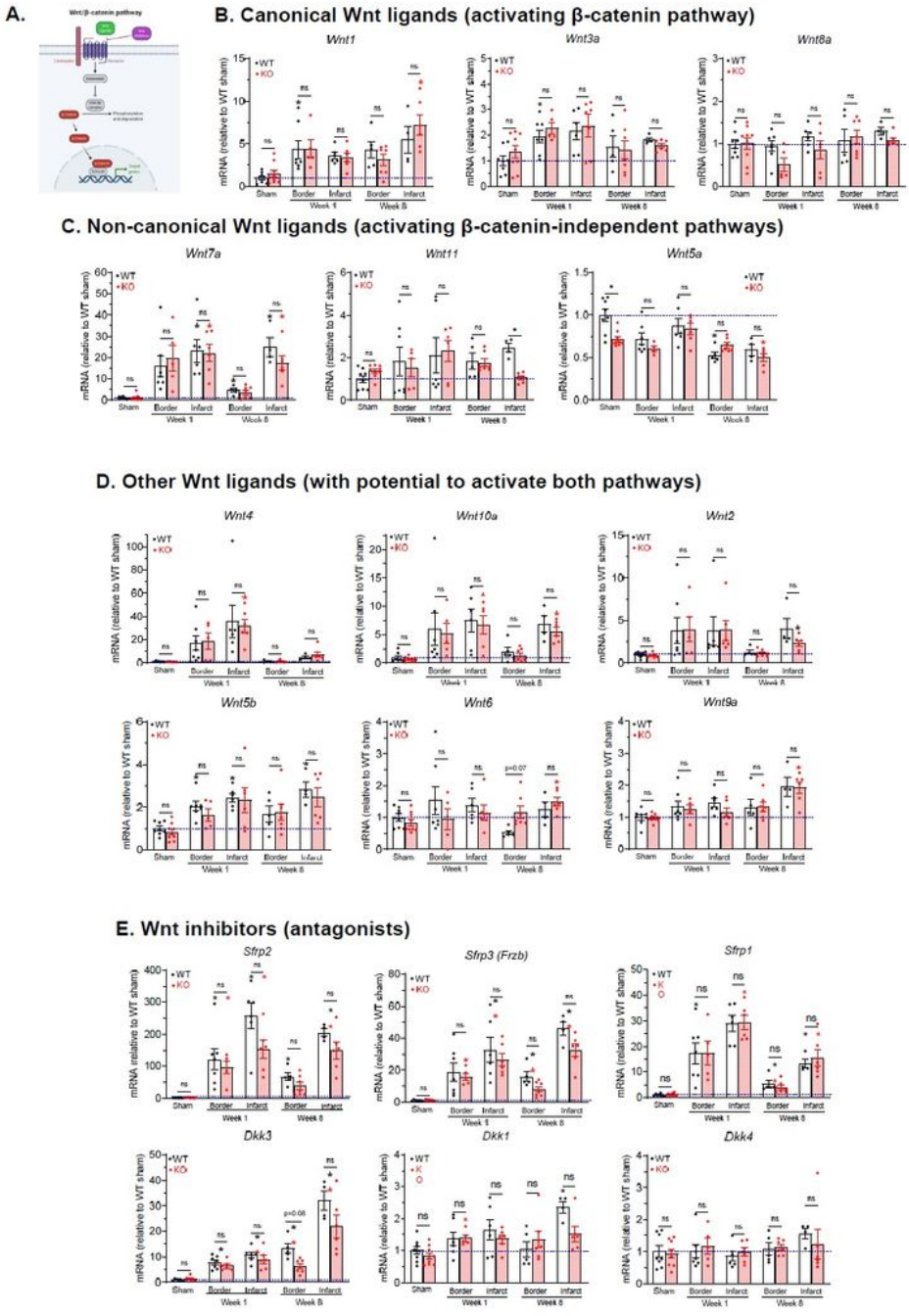

Figure 5

Both Wnt agonists and antagonists are upregulated at week 1 and 8 after myocardial infarction. A. Diagram of the canonical Wnt/β-catenin signaling pathway, which is fine-tuned by the soluble Wnt

ligands and inhibitors on the extracellular side of the plasma membrane. When a Wnt ligand binds to its plasma membrane receptor and co-receptor, it leads to the inhibition of GSK-3β which is the key component of the β-catenin degradation complex; β-catenin will accumulate in the cytoplasm and then translocate into the nucleus where it, together with TCF/LEF, activate or inhibit the transcription of target genes. Abbreviations: GSK-3β, glycogen synthase kinase 3β; TCF/LEF, T-cell factor/lymphoid enhancer factor. B to E. qRT-PCR analyses of transcript levels of canonical Wnt ligands (B), non-canonical Wnt ligands (C), other Wnt ligands that have been shown to activate both canonical and non-canonical pathways or have less defined actions (D), and Wnt ligand inhibitors/antagonists (E) in sham, 1-week post MI, and 8-week post MI infarct and border zone myocardium. n=4-10 per group. *$p<0.05$ vs. corresponding sham groups. “ns” means no significant difference between WT and KO groups. Data were analyzed by two-way ANOVA and Bonferroni post-hoc comparison.

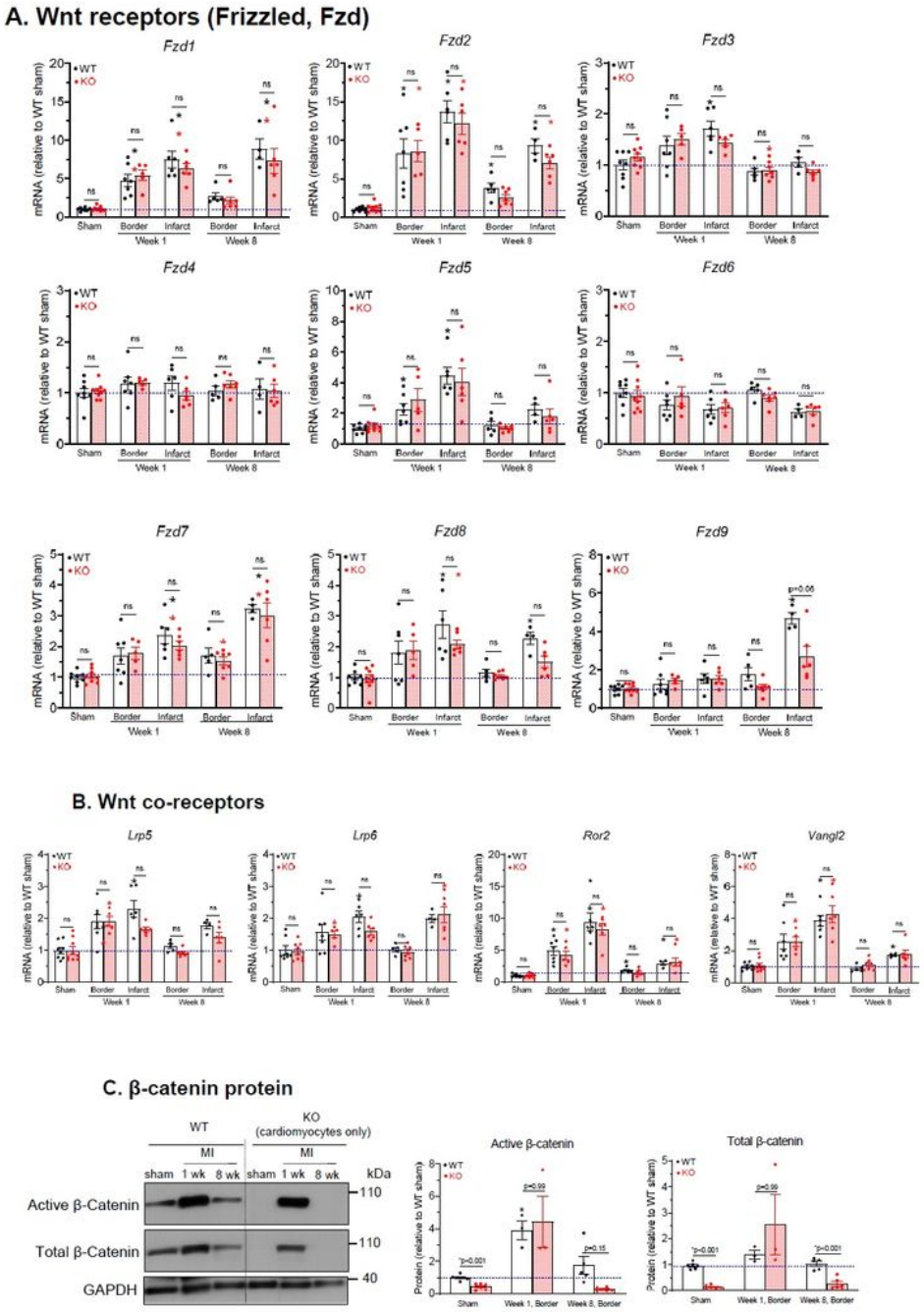

Figure 6

Wnt receptors and co-receptors are upregulated after myocardial infarction. A and B. qRT-PCR analyses of transcript levels of Wnt receptors (A), Wnt co-receptors (B) and Wnt target genes (i.e., genes known to be upregulated by Wnt/β-catenin pathway, panel C) in sham, 1-week post MI, and 8-week post MI infarct and border zone myocardium. n=4-10 per group. C. Western blot of border zone tissue (MI, n=3-6) or left ventricular anterior free wall (sham, n=5-6) with anti-non-phospho (active) β-catenin (Ser33/Ser37/Thr41)

antibody and anti-total β-catenin antibody. GAPDH was used as a loading control. The original uncropped gel images are included in Supplementary Figure 1. *p<0.05 vs. corresponding sham groups. “ns” means no significant difference between WT and KO groups. Data were analyzed by two-way ANOVA and Bonferroni post-hoc comparison.

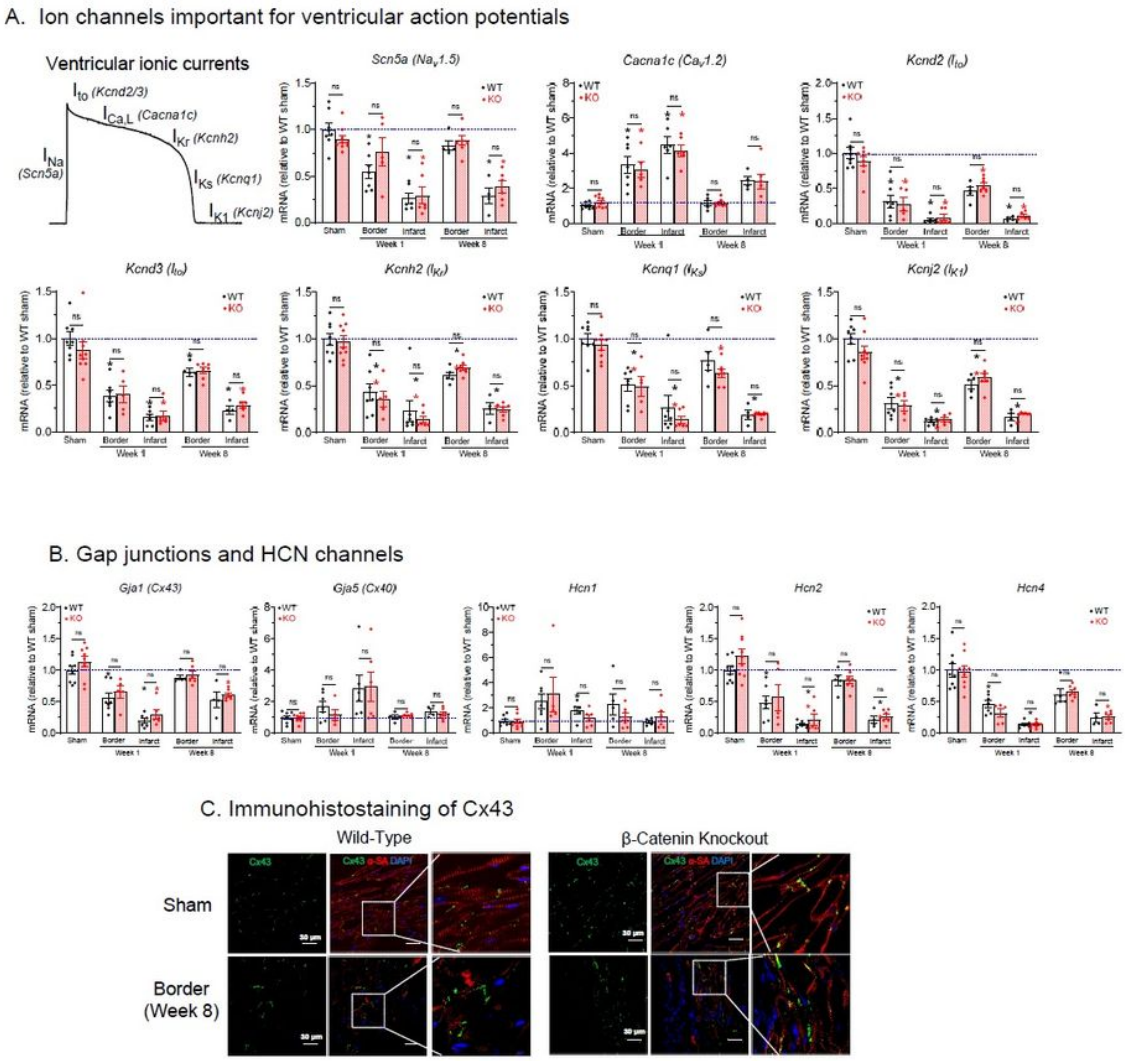

Figure 7

Ion channel gene expressions after myocardial infarction. A and B. qRT-PCR analyses of transcript levels of ion channels involved in ventricular action potentials (A), and gap junctions and HCN channels (B) in sham, 1-week post MI, and 8-week post MI infarct and border zone myocardium. n=4-10 per group. *p<0.05 vs. corresponding sham groups. “ns” means no significant difference between WT and KO groups. Data were analyzed by two-way ANOVA and Bonferroni post-hoc comparison. Abbreviations in

panel A: INa, cardiac sodium current; Ito, transient outward potassium current; ICa,L, L-type calcium current, IKr, rapidly activating delayed rectifier potassium current; IKs, slowly activating delayed rectifier potassium current; IK1, inwardly rectifying potassium current. C. Representative confocal images showing similar distribution patterns of Connexin 43 (Cx43, green) in WT and KO myocardium. In sham hearts (top panels) of both WT and KO groups, Cx43 is restricted to the cell-cell junctions. In the border zone of hearts at 8-week after MI (bottom panels), both WT and KO groups showed a more diffusive pattern for Cx43. Cells were co-stained with α-sarcomeric actinin (α-SA, red color, a marker of cardiomyocytes) and DAPI (blue).

Supplementary Files

This is a list of supplementary files associated with this preprint. Click to download.

- OnlineSupplementTableforqPCRprimers.pdf
- SupplementaryFigure1.pdf